UNIVERSITY OF GOTHENBURG

DEPARTMENT OF BIOLOGICAL AND ENVIRONMENTAL SCIENCES

LONG-TERM IMPACTS OF CLIMATE AND LAND USE CHANGE ON WATER AVAILABILITY OF TWO WATERSHEDS WITHIN THE UPPER BLUE NILE BASIN, ETHIOPIA

Momen Eshaq

Degree project for Master of Science (120 hec) with a major in Environmental Science

ES2500, Examination Course Environmental Science, 30 hec

Second cycle

Semester/year: Spring 2023

Supervisor: Annemieke Gärdenäs, Department of Biological and Environmental Sciences

Examiner: Johan Uddling Fredin, Department of Biological and Environmental Sciences

Acknowledgements

I would like to acknowledge that this thesis is based on several early publications and data produced by Annemieke Gärdenäs, Solomon Gebrehiwot, Per-Erik Mellander and many others; this project would not have been possible without their previous work.

I would also like to express my gratitude to everyone who supported me throughout this project. I thank my supervisor, Annemieke Gärdenäs, for her invaluable guidance, encouragement and feedback. She has been a great mentor and a source of inspiration for me. She also provided me with many insights and ideas for this project. I appreciate her patience and flexibility in accommodating my needs and preferences. I am also thankful to Solomon Gebrehiwot at Addis Ababa University for answering my questions regarding the study areas and Marc Vis at the University of Zurich for his advice on the HBV-light model.

I want to thank my opponent, and my examiner Johan Uddling Fredin, who gave constructive criticism and feedback on the thesis presentation and the report. Their contribution helped me to correct and clarify my report during the revision.

I appreciate the encouragement that I received from my friends. Especially when I faced challenges or difficulties, they helped me to stay positive and motivated.

Last, I want to acknowledge the Adlerbertska Foundations for awarding me the Axel Adler scholarship to pursue my studies at the University of Gothenburg. This scholarship enabled me to access high-quality education here. I am grateful to the scholarship team for their generosity and support. Without it, this educational journey would not have been possible.

Front Cover: Upper Blue Nile Basin and study watersheds delineated based on https://www.hydrosheds.org/

Abstract

The Upper Blue Nile Basin (UBNB) is undergoing significant land use change (LUC) due to agricultural expansion and deforestation. LUCs have implications for water resources in the region. Moreover, the UBNB is vulnerable to climate change (CC), which alters the hydrological regime and affects rainfall-dependent agriculture, increasing the risk of food insecurity during drought. The HBV-light and AquaCrop models were employed in two watersheds (Gilgel Abbay and Birr) in the UBNB to predict the impacts of these changes on water availability. The simulations were applied under baseline climate (1970 – 1999) and compared to a CC scenario (2070 – 2100). The parameters of LUC scenarios used in the HBV-Light were based on calibrated and validated water balance components of prominent historical trends in LUC (eucalyptus plantations and restoration of natural forests and wetlands). The HBV model's results were then analysed to calculate the water availability indicator, the ratio (0 to 1) of actual to potential evapotranspiration (AET/PET); a higher ratio value indicates more water availability.

In Gilgel Abbay, the ratio of AET/PET increased by 5.8% in CC with restoration LUC scenario compared to the baseline, and the number of days where the AET reached maximum PET (Ratio of >0.9) was higher by 137%. Both CC without LUC and with eucalyptus plantation had a reduction in the ratio of AET/PET, and the number of days (>0.9) decreased by -70% and -67%, respectively. In Birr, the CC without LUC had the highest increase in the number of days with >0.9 ratio, and the increase was by only 3%, while in restoration LUC, there was a decrease by -5%, and the most significant reduction was in the eucalyptus plantation scenario by -14%. It is worth noting that Birr generally did not have water stress since, in all scenarios, including the baseline, the ratio was over 0.9.

On the other hand, the AquaCrop was used to predict how commonly cultivated crop yields (Teff and Barley) in the UBNB are affected by the projected CC. The results showed that water is not limiting for the investigated crops. Instead, the yields are predicted to increase due to the increase in rainfall and CO_2 fertilisation during the growing season of those crops.

The results of this paper indicate that water availability in the investigated watersheds is significantly affected by LUC at the watershed scale. The applied land-use change scenarios can help inform future land management decisions to ensure water security, such as consideration of plans to expand the eucalyptus plantation.

Keywords: Land cover, land use, water management, hydrological modelling, crop production

Contents

1. Introduction

The hydrologic cycle at the local, regional, and global scales are strongly affected by anthropogenic-induced global change drivers of land use change (LUC) and climate change (CC) (Kayitesi et al., 2022; Loaiciga et al., 1996). These effects in the cycle are observed by changes in processes such as evaporation, transpiration, precipitation, runoff, and groundwater recharge. Rapid changes in the cycle cause unacclimated frequencies, occurrences, durations, and intensities of extreme hydrological events such as droughts, floods, and heavy precipitation (Caretta et al., 2022; Pörtner et al., 2022). Consequently, the water balance needed to sustain natural and human systems is disrupted, which can significantly damage human well-being, livelihoods, and the environment. In Africa, the impacts of CC have already resulted in significant losses and damages, such as water shortages, reduced food production, loss of lives, and biodiversity loss (Trisos et al., 2022). For instance, agricultural productivity had a severe loss of 34% influenced by CC since 1961 (Ortiz-Bobea et al., 2021), and by 2050, up to 921 million people in sub-Saharan Africa could be exposed to CC-related water stress (Trisos et al., 2022). Additionally, LUC may amplify the CC impacts on water resources by altering hydrological regimes due to changes in precipitation patterns, soil moisture, groundwater recharge, and streamflow (Te Wierik et al., 2022; van Luijk et al., 2013). The widespread and fast rate of LUC in Africa is directly driven by the cultivation of crops, extraction of wood, and construction materials at the expense of natural vegetation land (Hosonuma et al., 2012).

A similar trend in LUC is observed in Ethiopia, where an intensifying change of natural vegetation cover to cultivated land has been accelerated in the past decades (Belay & Mengistu, 2019; Birhanu et al., 2019; Gebrehiwot et al., 2014). The LUC and CC impacts on water availability become more critical when transboundary water resources are affected, such as the Ethiopian highlands' Upper Blue Nile Basin (UBNB) region (Obengo, 2016). It is one of the major river basins in Africa, and its precipitation accounts for over 50 per cent of the water flow to the Nile River passing through downstream countries Sudan and Egypt (Conway, 2000). The basin is particularly vulnerable to hydrological changes due to its importance for agricultural and socioeconomic development for millions of people sharing its water resources. Most of the cultivated land in the UBNB is rainfed and has little irrigation infrastructure (Worqlul et al., 2015). As a result, food insecurity becomes more likely in case of changes in hydrology, such as increased drought events (Trisos et al., 2022). People in countries downstream may also be affected (Awange, 2022; Yitayew & Melesse, 2011).

On that account, several studies with various methodologies and scenarios have been conducted to predict LUC and CC impacts on the water resources in the basin. For instance, Mellander et al., (2013) predicted the potential impacts of CC on seasonal and annual rainfall over the UBNB using a spatial model based on historical trends and a downscaled global General Circulation Model (GCM) between 2050 and 2100. Downscaling of GCMs leads to greater spatial resolution at a specific regional scale. The study demonstrated an increase of 6% in annual mean rainfall; however, this increase varies between different seasons and regions of the basin. The change in the seasonality of rainfall patterns was also found by WaleWorqlul et al., (2018), who also used a semi-distributed conceptual model called the HBV hydrology model to simulate changes in the streamflow and their results indicated a possibility of significant variability in streamflow where an increase is seen during dry seasons and a decrease in wet seasons by the end of the 21st century. Hydrological modelling at the watershed scale, such as rainfall-runoff modelling, can provide insights for appropriate water management strategies in changing climate. It also assesses other processes influencing water balance on land, which can be critical factors in controlling the hydrological behaviour of watersheds (Dwarakish & Ganasri, 2015). For instance, (Birhanu et al., 2019) investigated the impact of historical LUC at the watershed scale using the HBV model on the water balance components.

Contrary to the expected impact of LUC by the author on changes in hydrology, the HBV model indicated only a slight change in the water balance components (±5%). However, the author concluded that uncertainties encountered in the modelling process (e.g., model structure, LUC representation) could have masked the LUC impacts on hydrology. Other studies (Getachew & Manjunatha, 2021; Teklay et al., 2021) used different models to investigate and compare both CC & LUC scenarios' impacts on water balance components. Their results, in general, suggest that the impact of climate change on water balance components such as evapotranspiration and streamflow is relatively higher than the combined LUC & CC impacts. However, LUC scenarios influenced CC impacts differently. For instance, Getachew & Manjunatha, (2021) found that expanding forest and irrigation scenarios augmented increased evapotranspiration under warmer conditions due to CC. In contrast, the expansion of the agriculture scenario had a marginal decrease in evapotranspiration under CC conditions. Using model outputs under different LUC scenarios can provide useful information about how the contribution of different land use dynamics under CC conditions affects the water balance components (Teklay et al., 2021).

Considering that UBNB is a highly agricultural area and with the population growth in the region, the demand for cultivated land is expected to increase (Lemann et al., 2018). Thereby, in addition to studying changes in water balance components, it is essential to assess how the commonly cultivated crops in the UBNB region will respond to future CC. For instance, according to a study by Araya et al., (2015), Teff, a commonly cultivated crop in Ethiopia, could suffer from reduced production by the midcentury if appropriate adaptation measures are not taken. Other grown crops in the region may face a similar fate when it comes to yield potential under changing climate (Araya et al., 2023). To predict how crops will be impacted in the future, crop growth models such as AquaCrop can be utilised to simulate plant-environment interaction and estimate the yield of crops under different scenarios (Spitters, 1990).

A review paper by (Dile et al., 2018) on water resources research in the basin identified several gaps and suggestions for future research. The authors suggested applying a multidisciplinary approach to understanding the impacts on water resources, such as investigating multiple modelling outputs from different disciplines rather than focusing on one output. Moreover, they found that some studies generalised the results of their study watershed for the entire basin. However, since the UBNB differ significantly in spatial characteristics and land uses, research is needed in different watersheds with distinct land use dynamics and other spatial characteristics.

Therefore, the overall aim of this study is to improve the understanding of how different land uses and climate change affect water availability at different scales by the end of the 21st century using modelling for watersheds with different spatial characteristics in the UBNB. This is achieved by the following specific aims:

(1) Predict and compare the impact of different LUC scenarios on water availability under climatic change (2070 – 2099) of two watersheds using the HBV Hydrology Model

(2) Predict the impacts of change in water availability on the yields of two socioeconomically important crops in the Upper Blue Nile Basin (Teff and Barley) using the AquaCrop Model.

2. Materials and Methods

2.1. Study Design

The method employed in this study was computer-based modelling to test scenarios of climate and land use change. Simulations in model studies help explore the consequences of different decisions and actions since they can be repeated with different data inputs and parameters to test scenarios. The model's accuracy is tested by calibration and validation by comparing its predictions with actual observations. A baseline period of calibrated and validated data from previous studies (1970 – 1999) was used for identifying changes in future CC predictions and LUC scenarios (2070 – 2099). The selection of 30 years is based on the classical period for averaging climatic variables, as defined by the World Meteorological Organization (*WMO Guidelines on the Calculation of Climate Normals*, 2021). Therefore, it is important to note that all the results presented in figures and tables are yearly mean or monthly means of 30 years.

This study assesses the CC and LUC impacts on water availability at different scales. For this purpose, two different modelling approaches are used: the HBV model and the AquaCrop model. The HBV model simulates actual evapotranspiration (AET) and runoff using weather data and long-term potential evapotranspiration (PET) as inputs. PET is a measure of the ability of the atmosphere to remove water from a surface through evaporation and transpiration, while AET is the simulated quantity of water that has been removed from a surface (Pidwirny, 2006). In this study, PET refers to the reference evapotranspiration, while AET refers to the water removed from natural and agricultural systems at the watershed scale. Additionally, the 90% percentile of soil and groundwater statistics are computed by the HBV model, where they are split into three conceptual boxes one for soil water storage and two for groundwater storage (upper and lower).

The ratio between AET and PET is commonly used to indicate water availability, mainly for crop water demand (Brauman et al., 2013). AET reach PET when water is not limited, which means that the soil moisture and vegetation are sufficient to meet the atmospheric demand for water. When water is limited, actual evapotranspiration rates are lower than potential rates, creating a deficit between the demand and supply of water (Liu et al., 2017; Speich, 2019; Yao, 1974). The ratio (0 to 1) was used to indicate water availability in different scenarios and to calculate the number of days where the ratio reached its maximum (0>0.9).

On the other hand, the AquaCrop was used to simulate the yield potential with the baseline and future weather data to provide predictions on how water availability will affect crop production, which can be relevant to farmers on the field scale. The cumulative probability of yield potential is then calculated over the study period to predict if the commonly cultivated crops Teff (*Eragrostis tef*) and Barley (*Hordeum vulgare*) yields are impacted.

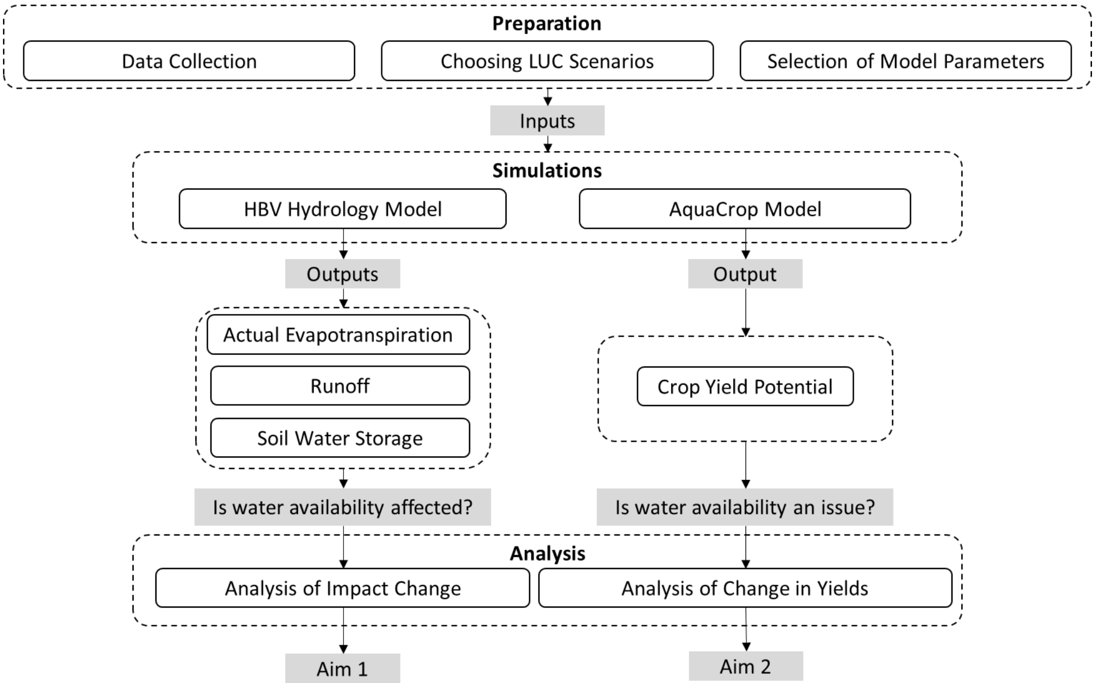

Figure 1
Schematic view of study design

2.2. Study Area Description

The Upper Blue Nile Basin region is home to several watersheds contributing to the Nile River basin. The region is a significant geological and hydrological feature of the northwestern Ethiopian Plateau, occupying about 17% of the country's land area. The UBNB extends from 7° 45′ to 12° 45′ N latitudes and 34° 05′ to 39° 45′ E longitudes. It covers three administrative regions of Ethiopia: Oromia, Amhara and Benishangul-Gumuz. The region has a varied landscape, climate, soil and vegetation types (Melesse et al., 2011). The climate is marked by seasonal changes in rainfall and the seasons are named according to these changes; Bega, the dry winter season (October – February); Belg, the small rains of spring (March–May); and Kiremt, the wet summer season (June–September) (Mellander et al., 2013). About 85% of the rainfall occurs between July and October (Ministry of Water and Energy, 2023). The two watersheds selected are Gilgel Abbay and Birr (figure 2). The main difference is the size; other differences include land use history (Table 1 and Section 2.5).

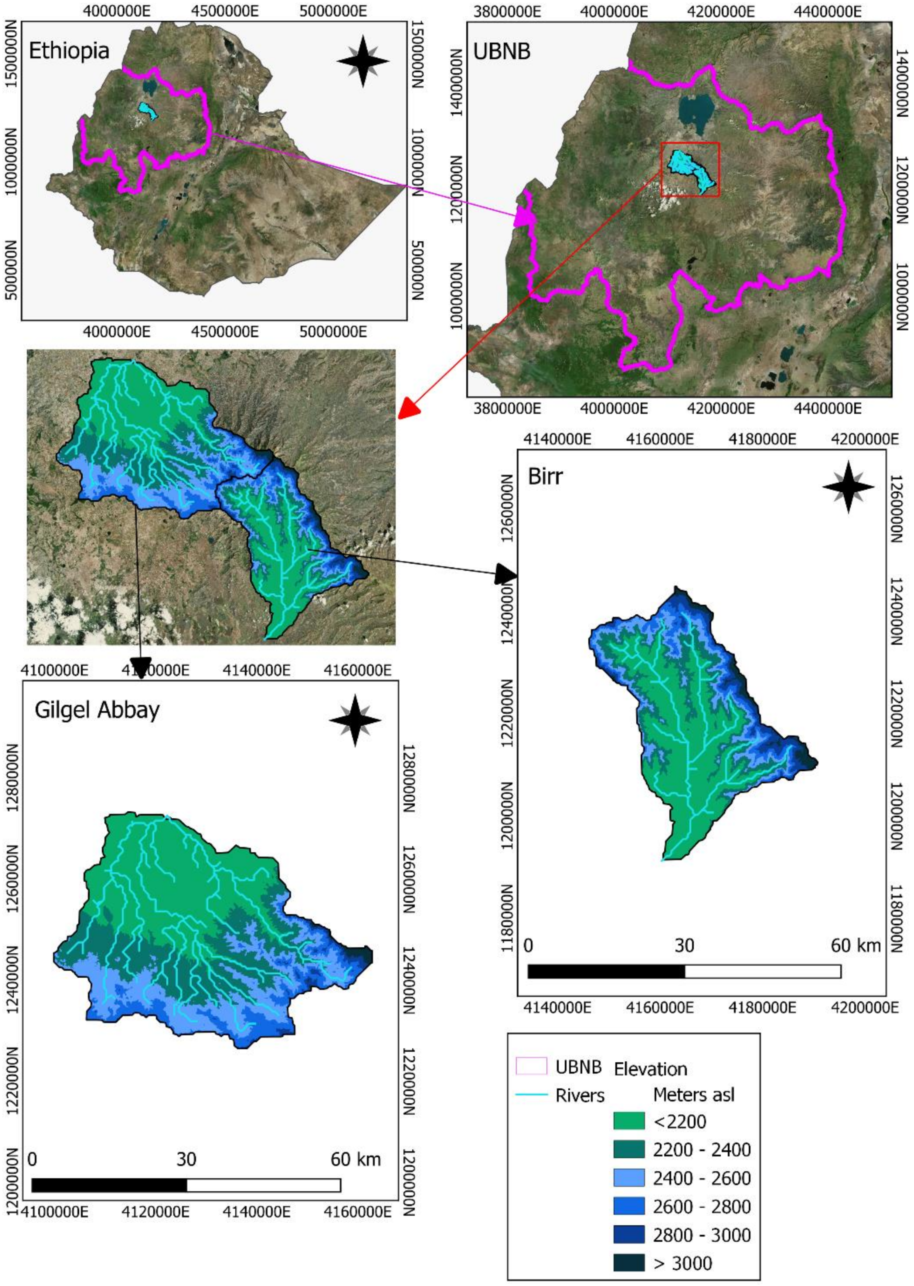

Figure 2

The geographical location of the study watersheds Gilgel Abbay and Birr in the Upper Blue Nile Basin

Table 1

Main watershed characteristics (Gebrehiwot et al., 2013)

	Area (km^2)	Mean Altitude (m)	Mean Annual Rainfall 1970 – 1999 (mm)
Gilgel Abbay	1660	1900	1514
Birr	980	1790	1693

2.3. Baseline Hydroclimate Data

Data including rainfall, temperature, potential evapotranspiration (PET), and streamflow for each watershed are needed to simulate the water balance components in the HBV Hydrology model. The baseline hydroclimate period data (1970 – 1999) was provided by Gebrehiwot et al., (2013). The authors received the daily rainfall and temperature data from The National Meteorological Service Agency of Ethiopia and estimated the climatic data for each watershed based on the means of nearby meteorological stations. The long-term monthly mean PET was estimated using the Hargreaves method (H. Hargreaves & A. Samani, 1985). This method is simple and widely used to estimate PET based on average, minimum and maximum air temperature and extraterrestrial radiation. Several studies have confirmed that the Hargreaves equation performs well for time steps of five days or longer (Droogers & Allen, 2002; Hargreaves & Allen, 2003; Patel et al., 2015).

2.4. Future Hydroclimate Data

For the future climate (2070 – 2099) simulations, weather data was provided by Mellander et al., (2013), which spatially and temporarily downscaled data based on a coupled climate model consisting of atmospheric and oceanic general circulation model (GCM) called ECHAM5/MP1-OM. GCMs are mathematical representations of the Earth's atmosphere, oceans, land, and ice. They simulate the interactions between these components and the effects of natural and human factors on the climate system. Using historical data and physical laws, climate models can project how the future climate will evolve under different greenhouse gas emissions scenarios and other forcings. The authors downscaled the ECHAM5/MP1-OM using observations made between 1952 and 2004 in 19 meteorological stations in the UBNB. The scenario for the downscaling ECHAM5/MP1-OM was based on the output prepared for the Intergovernmental Panel on Climate Change (IPCC) Fourth Assessment of the 20th Century experiment (20C3M). Scenario 20C3M assumed greenhouse gasses increased as observed through the 20th century (*Scenario Data for the Atmospheric Environment*, n.d.). PET for the future climate was estimated using the Hargreaves method (*Annemieke Gärdenäs, Jan 2023, personal communication*).

2.4.1. Change in Climatic Variables

The mean increase in temperature for the 30-year periods rose by around 0.5 °C for Gilgel Abbay and Birr (Table 2). June had the highest increase (0.7 °C), and April had the lowest (0.15 °C) in both watersheds (Figures 3 & 4). The annual total precipitation based on 30-year mean precipitation increased by 30.9 (2.05%) mm in Gilgel Abbay and 55.4 (3.27%) mm in Birr (Table 3). Overall precipitation increased in all seasons but differed between the months of the seasons. For example, During the Belg, the precipitation increased in the middle of the season (April), while it decreased in May in both watersheds. Similarly, in the rainiest Kiremt season, there was a decrease in June while increasing in August. The Bega season showed a trend of increased precipitation in all the months (Figures 3 & 4).

Table 2

Yearly temperature (absolute values and percentage of change)

	Gilgel Abbay		Birr	
	Baseline	CC	Baseline	CC
Absolute values (°C)	19.16	19.64	16.12	16.57
% of change	+2.52%		+2.79%	

Table 3

Yearly precipitation (absolute values and percentage of change)

	Gilgel Abbay		Birr	
	Baseline	CC	Baseline	CC
Absolute values (mm)	1514	1545	1693	1748
% of change	+2%		+3.3%	

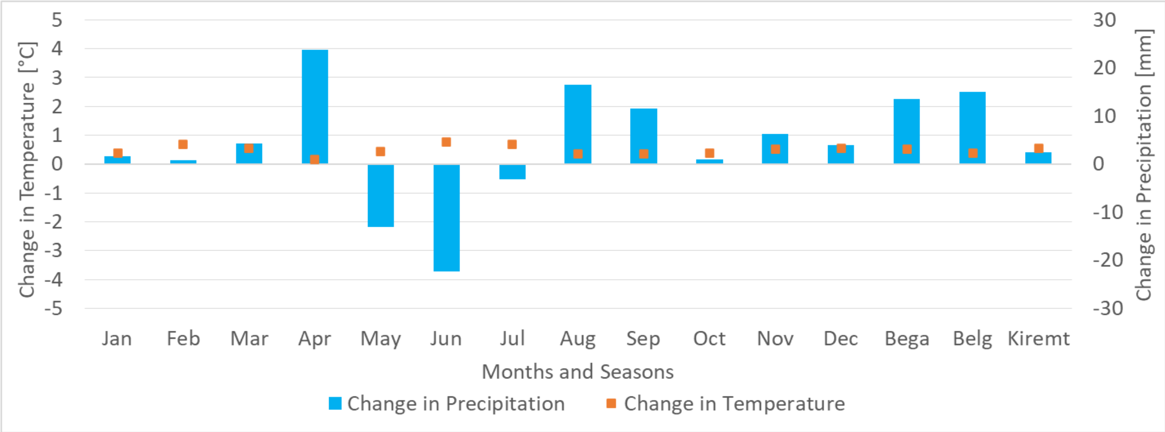

Figure 3

Monthly and seasonal changes in temperature and precipitation in Gilgel Abbay watershed

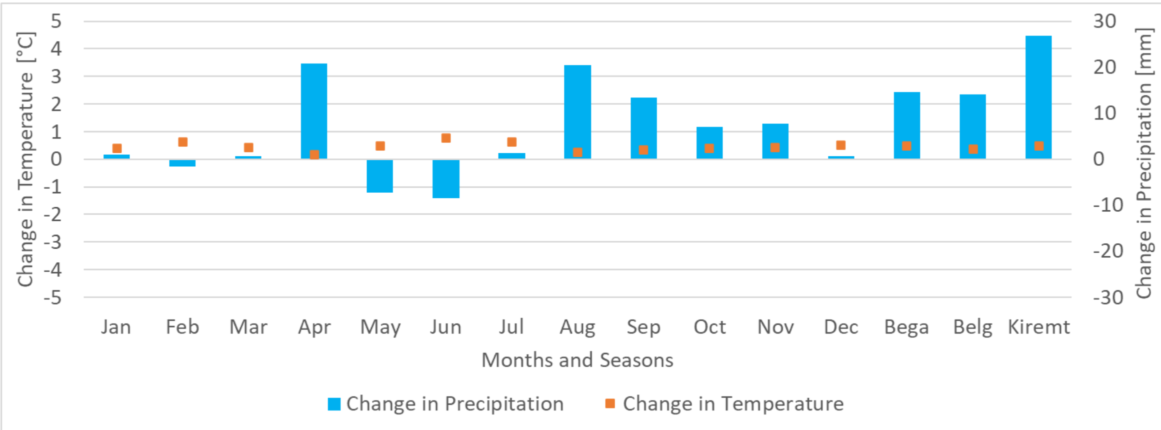

Figure 4

Monthly and seasonal changes in temperature and precipitation in Birr watershed

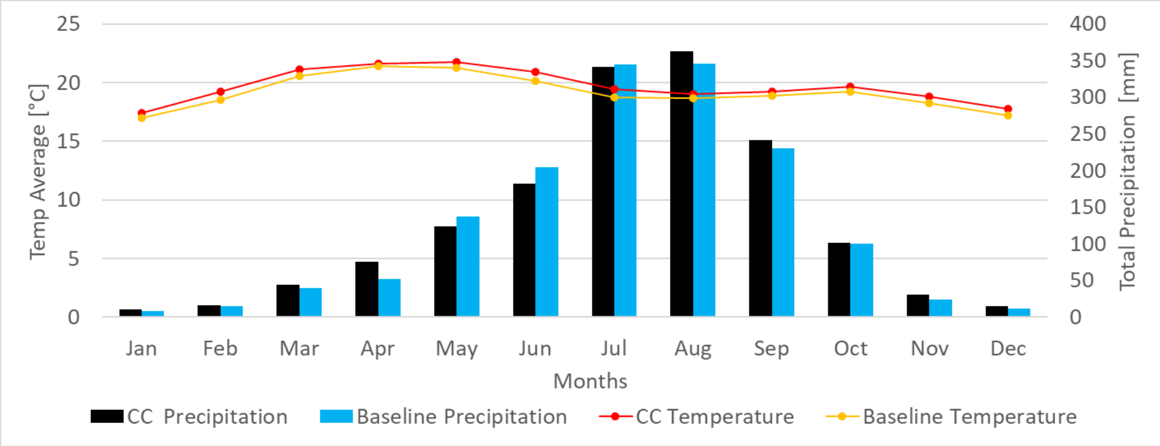

Figure 5

Absolute values of average monthly temperature and precipitation (Baseline and CC) in Gilgel Abbay watershed

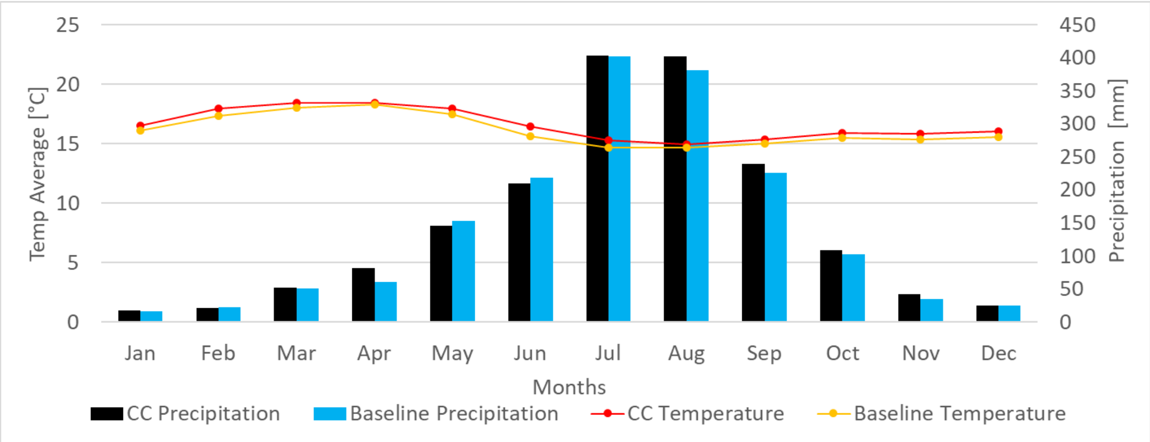

Figure 6

Absolute values of average monthly temperature and precipitation (Baseline and CC) in Gilgel Abbay watershed

2.5. Land Use Change Scenarios

LUC data of the two watersheds is based on the historical trends and findings by Gebrehiwot et al., (2014). The paper identified nine types of LUC, including five natural covers, and compared the change over four decades (1957-2001) using aerial photographs and satellite images. One of the authors' findings is that natural forest cover decreased in all watersheds, and natural riverine forests have disappeared since 1975, while eucalyptus plantations were intensified in both watersheds during 1991-2004. Agriculture and bushlands remained the dominant land-use type occupying more than half of the total land area in both watersheds. In this paper, the relevant periods used as the baseline of the land use and the scenarios are based on these historical trends specific to the watersheds (Figures 7 and 8). Due to the availability of calibrated and validated parameters for the modelling, these LUC trends are useful to provide insights into how watershed hydrology behaves with future CC. The baseline land cover is based on the period between 1976-1990, which reflect the most likely land use during the baseline climate period (1970 – 1999). The LUC Scenario 1 (Eucalyptus) is based on the changes between 1991-2004, which were characterised by an increase in eucalyptus plantations, while LUC Scenario 2 (Restoration) is based on earlier identification of land cover between 1960-1975, characterised by higher natural forest cover.

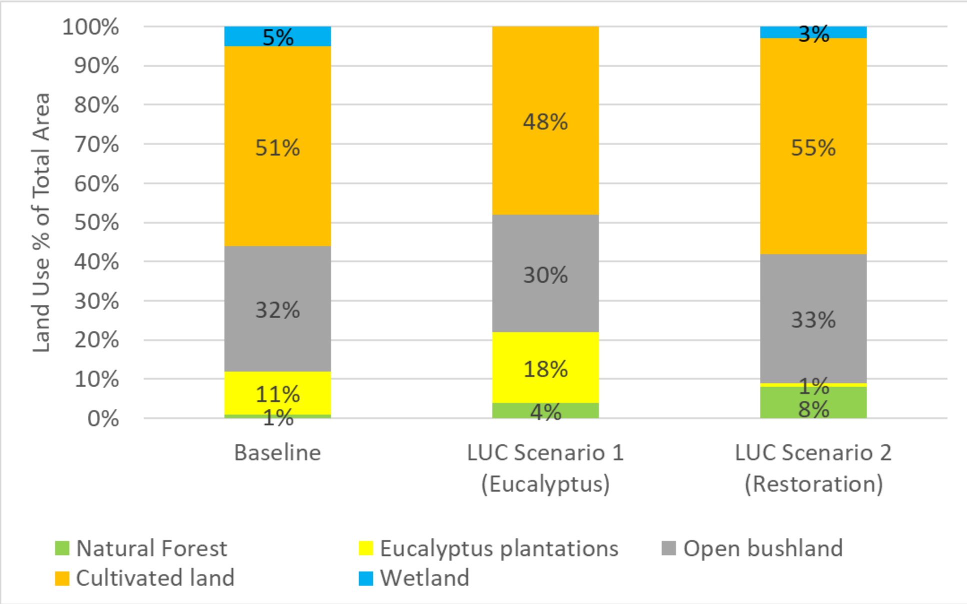

Figure 7

Percentage of land use for the Baseline, LUC Scenario 1 (Eucalyptus), and LUC in Scenario 2 (Restoration) in Gligel Abbay Watershed (Gebrehiwot et al., 2014)

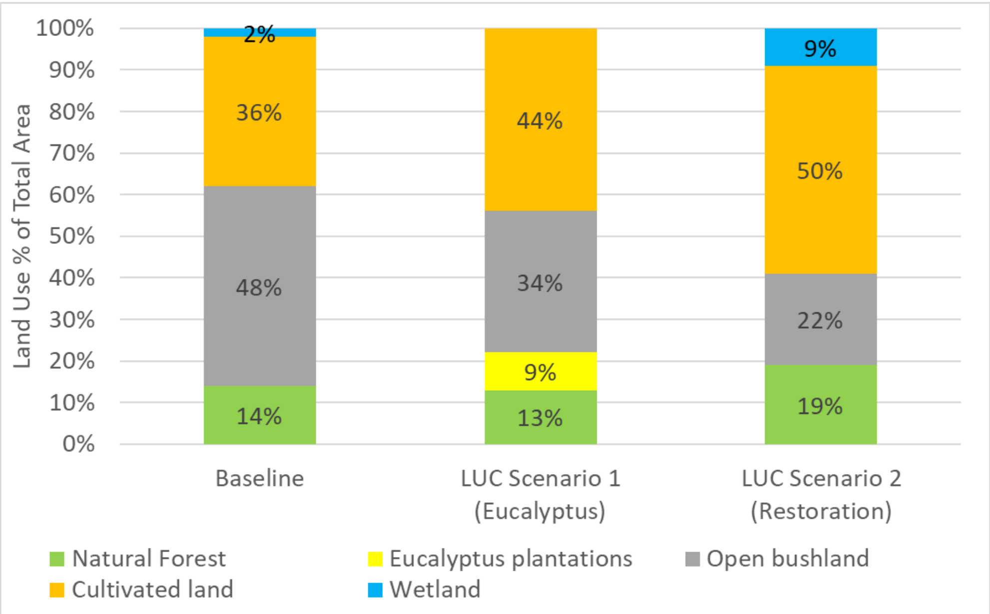

Figure 8

Percentage of land use for the Baseline, LUC Scenario 1 (Eucalyptus), and LUC in Scenario 2 (Restoration) in Birr Watershed (Gebrehiwot et al., 2014)

2.6. Hydrological Modelling

2.6.1. The HBV Model Description

It is a conceptual rainfall-runoff semi-distributed hydrological model originally developed by the Swedish Meteorological and Hydrological Institute (SMHI) in the 1970s to assist hydropower operations in Sweden. Since then, it has been further developed (Seibert & Bergström, 2021), and its applications in hydrological studies include water balance prediction and the effects of climate change, among others (Bergström, 1992). The model's applicability for simulating climate change impacts on water balance components was successful in several locations worldwide (Abdo et al., 2009; Crossman et al., 2013; Pervin et al., 2021; Steele-Dunne et al., 2008; WaleWorqlul et al., 2018). In the 1990s, a version of the model called HBV-light was developed at Uppsala University with the purpose of providing a user-friendly interface version for research and education (Seibert & Vis, 2012). The model consists of multiple routines, the soil routine, the groundwater routine, and the routing routine. In addition, there is the snow routine which was not considered in this study. Figure 9 illustrates the structure of the HBV model, including the parameters relevant to each routine. A description of the parameters relevant to the study watersheds and their units can be found in Table 4. The version of HBV-light used in this study was 4.0.025, developed at the University of Zurich and downloaded from the web link https://www.geo.uzh.ch/en/units/h2k/Services/HBV-Model/HBV-Download.html.

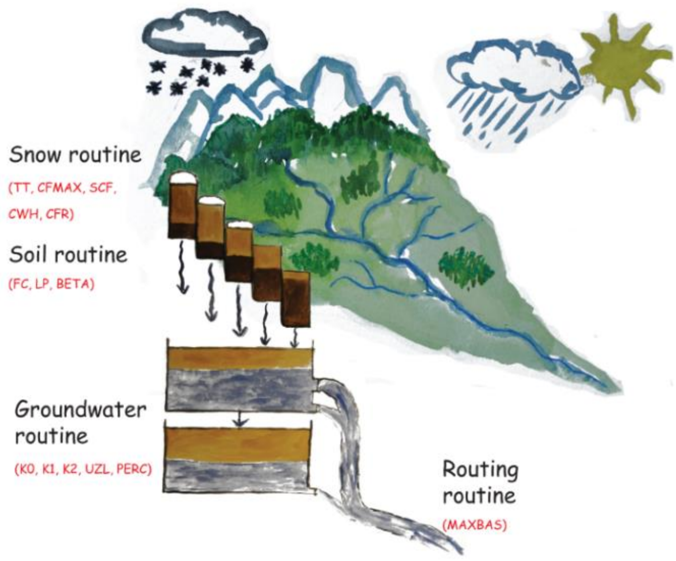

Figure 9

Structure of the HBV model and parameters in red colour retrieved from (Seibert & Vis, 2012)

Table 4

Parameters of the HBV Model

Abbreviation	Unit	Description
FC	mm	Maximum soil moisture storage
LP	-	Threshold parameter for soil moisture value above which actual evapotranspiration reaches potential evapotranspiration
BETA	-	A coefficient parameter that determines the relative contribution to Runoff from rain or snowmelt
PERC	mm/Δt	Threshold parameter for maximum percolation from upper to lower groundwater storage
UZL	Mm	Threshold parameter for quick Runoff for k0 outflow
K0	1/Δt	Storage (or recession) coefficient 0
K1	1/Δt	Storage (or recession) coefficient 1
K2	1/Δt	Storage (or recession) coefficient 2
MAXBAS	Δt	Routing, length of the triangular weighting function

2.6.2. Model and Watershed Settings

The HBV-light has different options for model structure; the standard version basic model was used. In the simulation options, the HBV-light uses a warm-up period during which the watershed variables evolve from standard initial values to appropriate values according to meteorological conditions and parameter values. This period is not considered in the results. Five years of time series data between the 1st of January 1965 and the 31st of December 1969 for the baseline period was used as the warming-up period. Similarly, the 1st of January 2065 to the 31st of December 2069 was used for future climate change simulations.

2.6.3. Parameterization for Land Use Scenario

Calibrated and validated HBV model parameters mentioned in Table 4 for each watershed were provided by Gebrehiwot et al., (2013). The author used the Monte Carlo mathematical optimisation approach to generate the 50 best parameter sets for three periods between 1960–2004. Those 50 sets were chosen based on the highest Nash-Sutcliffe efficiency (NSE) values (>0.6) from two hundred fifty thousand runs (Gebrehiwot et al., 2013). The Nash–Sutcliffe efficiency measures how well a model simulates the observed data. If NSE = 1, the model perfectly predicted the observed data, while NSE less than 0 indicate that the model cannot predict the observed data. The choice of parameter sets for each land use scenario (Figures 7 and 8) was made by matching them with a corresponding period that reflected the classified land uses identified. This approach ensured that the parameter sets were consistent with the observed land use changes and captured the effects of different land use dynamics on the hydrological processes. In Table 5, a summary of the land use periods and their parameter sets median values are given. Each value in the table represents the median of the 50 best values.

Table 5

The land use scenarios and median values of the corresponding 50 best parameter sets (Gebrehiwot et al., 2013, 2014).

Watershed/LU Scenarios	Period	FC	LP	BETA	PERC	UZL	K0	K1	K2	MAXBAS
Gilgel Abbay / Restoration Scenario	1960-1975	196	0.86	2.40	4.17	75.51	0.09	0.05	0.09	2.24
Gilgel Abbay / without LUC Reference	1976-1990	227	0.94	1.68	4.20	73.93	0.09	0.09	0.10	2.54
Gilgel Abbay / Eucalyptus Scenario	1991-2004	217	0.95	1.80	3.38	76.75	0.18	0.09	0.10	1.89
Birr / Restoration Scenario	1960-1975	1208	0.21	1.15	2.94	43.98	0.24	0.22	0.13	1.96
Birr / without LUC, Reference	1976-1990	1387	0.17	1.10	2.78	55.52	0.28	0.25	0.12	2.41
Birr / Eucalyptus Scenario	1991-2004	1605	0.28	1.10	1.66	61.51	0.24	0.21	0.12	2.73

Table abbreviation: FC, maximum soil moisture storage. LP, threshold parameter for soil moisture value above which actual evapotranspiration reaches potential evapotranspiration. BETA, a coefficient parameter that determines the relative contribution to runoff from rain. PERC, threshold parameter for maximum percolation from upper to lower groundwater storage. UZL, threshold parameter for quick Runoff for k0 outflow. K0, K1, K2, Storage (or recession) coefficient. MAXBAS, routing, length of the triangular weighting function

2.7. Crop Growth Modelling

2.7.1. The AquaCrop Model Description

AquaCrop is a model to simulate herbaceous crop growth and yields developed by The Food and Agriculture Organization (FAO), and it is a water-driven process-based multi-simulation model (Vanuytrecht et al., 2014). The model can simulate yields under various environmental conditions using conservative crop parameters (constant with time, management practices, and geographic location) and non-conservative crop parameters (affected by the climate, field management or conditions in the soil profile). The version used is 7.0 (August 2022) and downloaded from https://www.fao.org/aquacrop/software/en/.

2.7.2. Climate Data

In addition to the precipitation and temperature data, the model requires reference evapotranspiration (ET_o) and atmospheric CO_2 concentrations. It is recommended to use the FAO Penman-Monteith equation to calculate ET_o. This equation determines the ET_o from meteorological data and a hypothetical grass reference surface (FAO, 2015). However, in this study, the Hargreaves method used for calculating PET in the HBV model was also used as input in AquaCrop as ET_o. The Hargreaves method has shown reasonable ET_o results with a global validity (Allan et al., 1998, p. 56; M et al., 1992). Daily precipitation and ET_o, monthly maximum and minimum temperatures files were created. Regarding CO_2 concentrations, simulations were done without and with changes in CO_2. That is to understand the impacts without the influence of CO_2 fertilisation on yields since atmospheric CO_2 concentrations are well documented to increase yields (Ainsworth & Long, 2005). Additionally, simulations with the default AquaCrop CO_2 concentrations, as observed and predicted by measurements at Mauna Loa Observatory in Hawaii, U.S.A (1902 to 2100), were used to investigate the variability in yields due to CO_2 fertilisation.

2.7.3. Crop Parameters

For the conservative and non-conservative crop parameters, AquaCrop software has default calibrated data files for Teff (*Eragrostis tef*) and Barley (*Hordeum vulgare*) in Ethiopia (Araya, Habtu, et al., 2010; Araya, Keesstra, et al., 2010). The parameters were used in this study with the following assumptions for the non-conservative parameters.

- The planting method is direct sowing. Therefore, the size of the germinating seedling canopy is the default, and there is no requirement for adjustment.
- Initial canopy cover at 90% emergence is estimated as 1.5% for Teff and 3.56% for Barley
- The maximum canopy cover at the middle of the growing season reaches 81% for Teff and 80% for Barley as the default.
- The mode of crop canopy development is adjusted to the temperature regime of different years (Growing degree-days) rather than specific calendar days.
- No cultivar class changes in the plant's genetic traits and characteristics due to plant breeding and biotechnology. Therefore, cultivar class parameter values are the default.

Lists of crop parameters values are available in Appendix 1

2.7.4. Soil Parameters

The soil data were obtained from the Harmonized World Soil Database (HWSD) Viewer version 1.21, a tool developed by FAO to provide access to comprehensive global soil information. The HWSD Viewer allows users to select and download soil data based on specific coordinates, and it comprises a 30-arc-second (or ~1 km) raster image and an attribute database. Based on the identified watershed boundaries (figure 9), a shape file overlay was used to map the relevant soil in the study areas. 3 dominant soil groups were identified: Luvisol, Nitisol and Vertisol. 4 dominant soil characteristics profiles were found, 2 in the Luvisol group and 1 in each Nitisol and Vetisol. Each soil profile in the database has different soil characteristics values, such as fractions of sand, clay and soil depth. The soil profile information with database ID 17008 (Table 7) was chosen in this study due to its prevalence in both watersheds (Figure 10). To estimate soil water characteristics needed in AquaCrop, the calculator developed by the U.S. Department of Agriculture (USDA) was used, and information such as volumes of soil water content conditions for field capacity (FC), wilting point (WP), and maximum water holding capacity of the soil (Sat) was generated (Table 6). WP is when the soil is dry, and the plants cannot extract water from it. Field capacity is when the soil has enough water to support optimal plant growth but not so much that it causes waterlogging or runoff. Saturation is when the soil is completely filled with water, and additional water will either run off or drain through the soil. Total available water (TAW) in millimetres for plants is calculated automatically by AquaCrop based on these parameters.

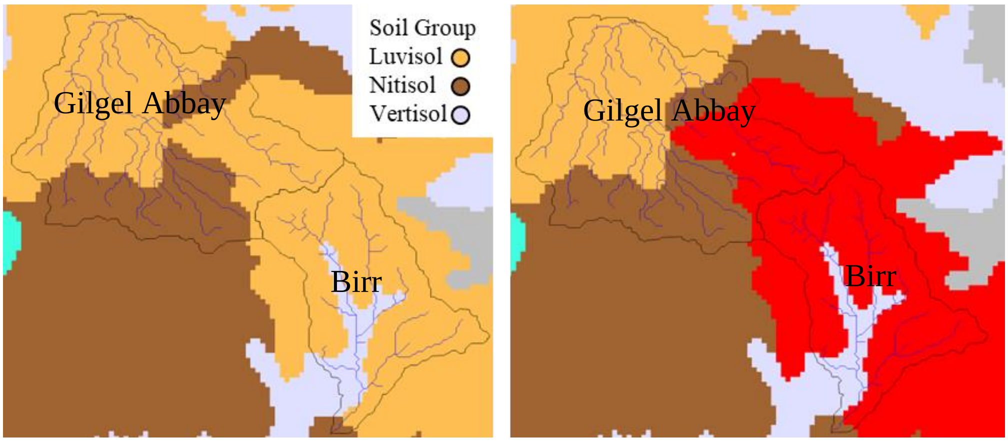

Figure 10

Dominant Soil groups map (left) and the identified prevalent soil profile in both watersheds with Database ID 17008 in red (right) (Nachtergaele et al., 2012)

Table 6

Main soil water characteristics needed in AquaCrop

	Saturation (Sat)	Field Capacity (FC)	Wilting Point (WP)	Saturated Hydraulic Conductivity of Soil (Ksat)
		vol %		(mm/day)
Topsoil	44	29	18	206
Subsoil	45	33	22	97

Table 7

Information Obtained from Harmonized World Soil Database (HWSD) for soil profile with Database ID 17008

Dominant Soil Group	LV - Luvisols
HWSD Database ID	17008
Topsoil Sand Fraction (%)	51
Topsoil Silt Fraction (%)	22
Topsoil Clay Fraction (%)	27
Topsoil USDA Texture Classification	sandy clay loam
Topsoil Reference Bulk Density (kg/dm3)	1.38
Topsoil Bulk Density (kg/dm3)	1.45
Topsoil Gravel Content (%)	1
Topsoil Organic Carbon (% weight)	0.63
Topsoil pH (H2O)	6.4
Topsoil Salinity (ECe) (dS/m)	0
Subsoil Sand Fraction (%)	45
Subsoil Silt Fraction (%)	21
Subsoil Clay Fraction (%)	34
Subsoil USDA Texture Classification	clay loam
Subsoil Reference Bulk Density (kg/dm3)	1.33
Subsoil Bulk Density (kg/dm3)	1.5
Subsoil Gravel Content (%)	1
Subsoil Organic Carbon (% weight)	0.35
Subsoil pH (H2O)	6.5
Subsoil Salinity (ECe) (dS/m)	0

2.7.5. Growing Period

Initially, choosing the months when farmers start sowing was based on the literature review of crop growing periods (Minta et al., 2014), which was August for Teff and June for Barley. AquaCrop can automate the sowing date for consecutive years based on the amount and days of rainfall. The model is set to search and predict sowing dates during the months found in the literature and accumulated rainfall of 150 mm in the climate files. Harvesting dates were based on the calibrated growing days (Araya, Habtu, et al., 2010; Araya, Keesstra, et al., 2010), which then was converted to growing degree days (GDD) by AquaCrop. The GDD are the heat units (°C) that the crop accumulates in a day. They are calculated by subtracting the base temperature from the average air temperature. Each simulation had a different date for harvesting, depending on when the crop reached maturity.

2.8. Handling of Issues with Data

In Birr, there was missing precipitation data for 17 days out of a total of 12783 days (0.13%) in the period 1965 to 1999, and it was assumed that no rain occurred during those days. The year 2091 had 57.9% less precipitation (565 mm) than the baseline year 1991 (1343 mm). This seemed inaccurate since all other years had an increase in precipitation when compared to the baseline. Therefore, the amount of precipitation for 2091 was corrected by using the coefficient of determination of the regression for the other years and extrapolating the daily precipitation for the year 2091.

3. Results

3.1. Yearly Changes in Water Balance Components

In Gilgel Abbay, simulated actual evapotranspiration (AET) increased in all scenarios. The combined CC and restoration LUC scenario had a 20% increase compared to the baseline, which was more by 6% than the CC impact alone. The difference between CC alone and CC plus eucalyptus scenario was 2%. The runoff decreased in all scenarios, with the highest decrease in CC and restoration LUC scenario (11.6%), more than half of the other two scenarios (Table 8). Similarly, AET in Birr increased in all scenarios with variation between LUC scenarios. However, the highest increase was in CC without LUC (5%). Overall compared to Gilgel Abbay, Birr had less increase in AET. The runoff increased in both LUC scenarios but decreased in CC without LUC scenarios. The highest increase in runoff was in the CC & Eucalyptus LUC Scenario (10.4%) (Table 9).

The restoration scenario had a positive impact on the AET/PET ratio in Gilgel Abbay, increasing it by about 6% from the baseline. The other two scenarios, CC without LUC and Eucalyptus, had a reduction in the ratio by about 3%. The restoration scenario also increased the number of days with maximum AET potential by 137% compared to the baseline, while the other two scenarios decreased it by 70% and 67%, respectively (Table 8). In Birr, the AET/PET ratio did not change much from the baseline in any of the scenarios, except for a 14% decrease in the number of days with maximum AET potential (Table 9).

Table 8
Simulated yearly water balance components (absolute values and percentage of change) in Gilgel Abbay

		Baseline	CC without LUC	CC & Eucalyptus LUC Scenario	CC & Restoration LUC Scenario
Precipitation	Absolute values (mm)	1514	1545		
	% of change	--	+2%		
AET	Absolute values (mm)	620	704	697	744
	% of change	--	14%	12%	20%
Runoff	Absolute values (mm)	894	841	848	801
	% of change	--	-5.9%	-5.5%	-11.6%
Soil Water Storage	Absolute values (mm)	197	190	182	152
	% of change	--	-3.5%	-7.8%	-23%
Groundwater Recharge	Absolute values (mm)	2.5	2.3	2.3	2.1
	% of change	--	-6%	-6%	-13%
Groundwater Storage (Upper)	Absolute values (mm)	38	34	38	45
	% of change	--	-11%	0.3%	18%

Groundwater Storage (Lower)	Absolute values (mm)	32	32	25	34
	% of change	--	0	-22%	6%
AET/PET Ratio	Min=0, Max=1	0.54	0.52	0.53	0.57
	% of change	--	-3.5%	-3.2%	5.8%
Maximum AET/PET Ratio (>0.9)	Number of days	37	11	12	88
	% of change	--	-70%	-67%	137%

Table 9

Simulated yearly water balance components (absolute values and percentage of change) in Birr

		Baseline	CC without LUC	CC & Eucalyptus LUC Scenario	CC & Restoration LUC Scenario
Precipitation	Absolute values (mm)	1693	1748		
	% of change	--	+3.3%		
AET	Absolute values (mm)	1210	1273	1214	1236
	% of change	--	5%	0.4%	2%
Runoff	Absolute values (mm)	484	476	534	512
	% of change	--	-1.6%	10.4%	5.9%
Soil Water Storage	Absolute values (mm)	677	628	727	607
	% of change	--	-7%	7%	-10
Groundwater Recharge	Absolute values (mm)	16.6	15.6	17.3	16.6
	% of change	--	-6%	4%	0%
Groundwater Storage (Upper)	Absolute values (mm)	5	4	9	5
	% of change	--	-19%	75%	-4%
Groundwater Storage (Lower)	Absolute values (mm)	20	19	14	17
	% of change	--	-3%	-27%	-13%
AET/PET Ratio	Min=0, Max=1	0.94	0.95	0.91	0.93
	% of change	--	1.1%	-2.6%	-1.0%
Maximum AET/PET Ratio (>0.9)	Number of days	297	306	254	284
	% of change	--	3%	-14%	-5%

3.2. Monthly Changes in Water Balance Components

On monthly time scales, changes were plotted (Fig 10 – 16). These changes are based on the 30-period means compared to the baseline.

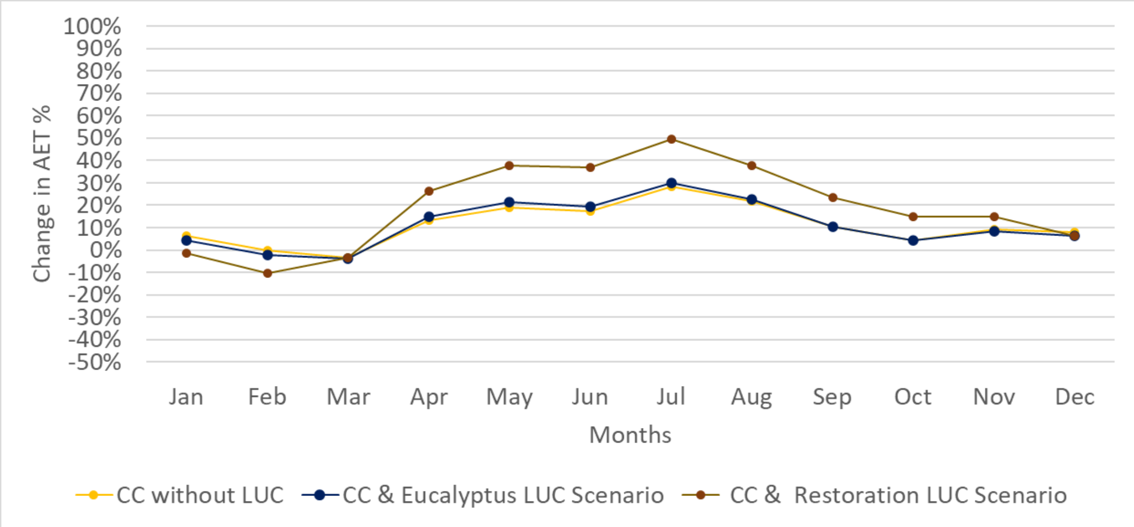

Figure 10

Simulated Monthly AET Change in Gilgel Abbay Watershed

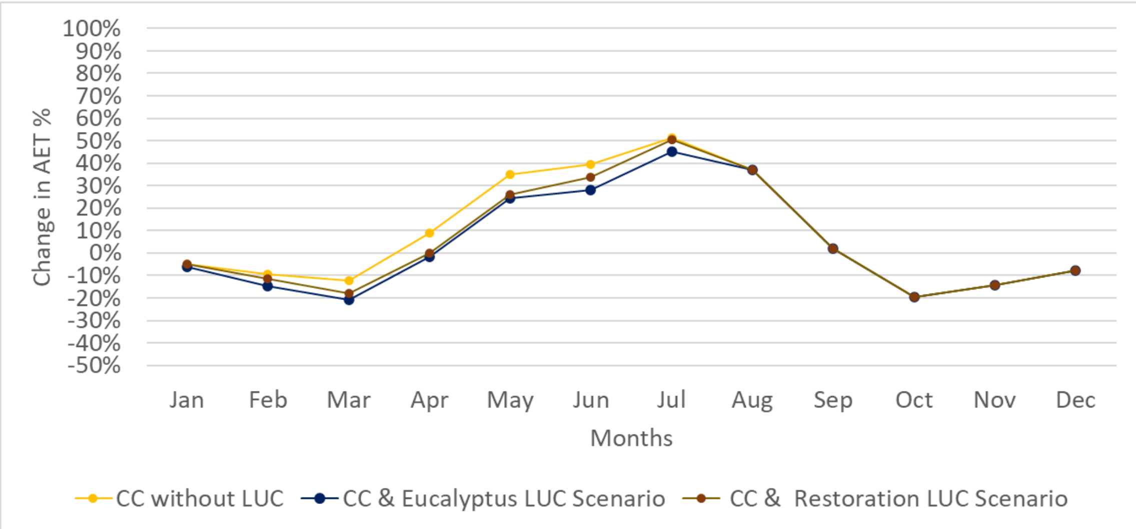

Figure 11

Simulated Monthly AET Change in Birr Watershed

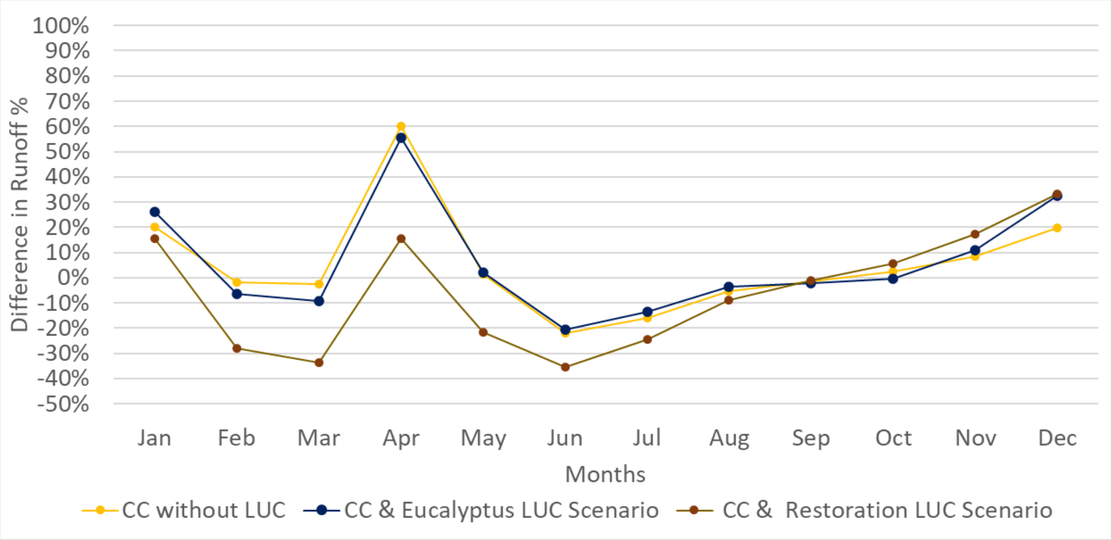

Figure 12

Simulated Monthly Runoff Change in Gilgel Abbay Watershed

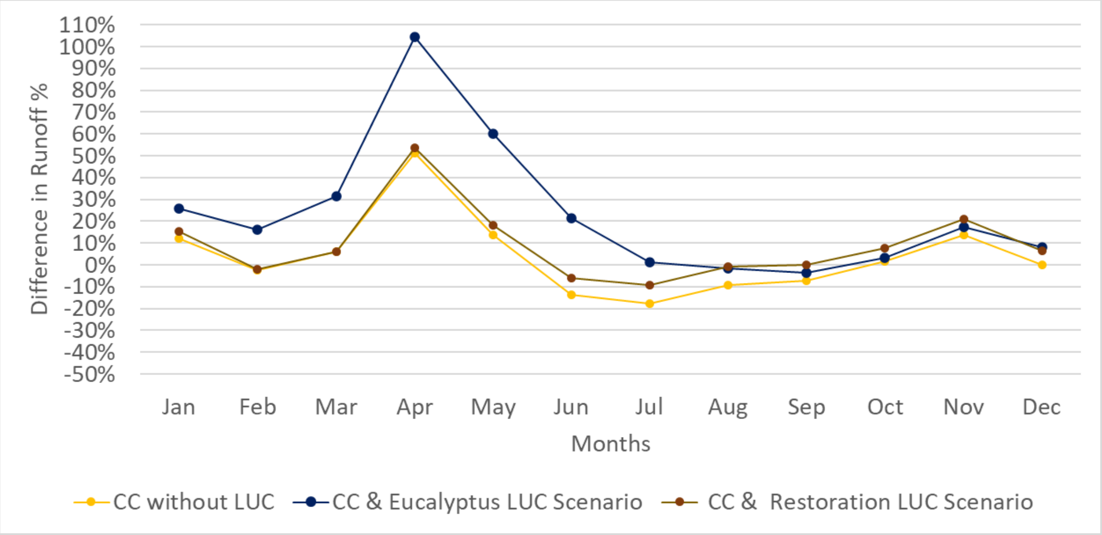

Figure 13

Simulated Monthly Total Runoff Change in Birr Watershed

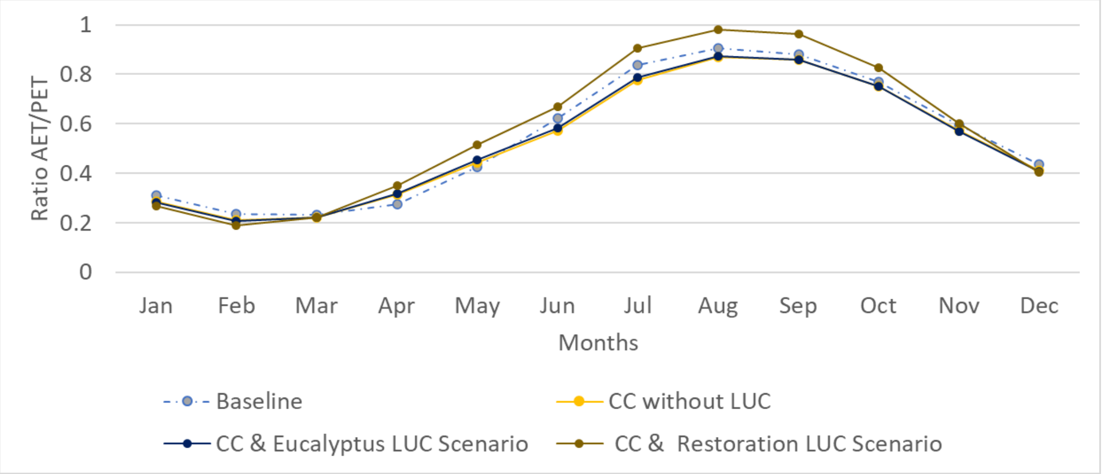

Figure 14

Simulated monthly AET/PET Ratio in Gilgel Abbay

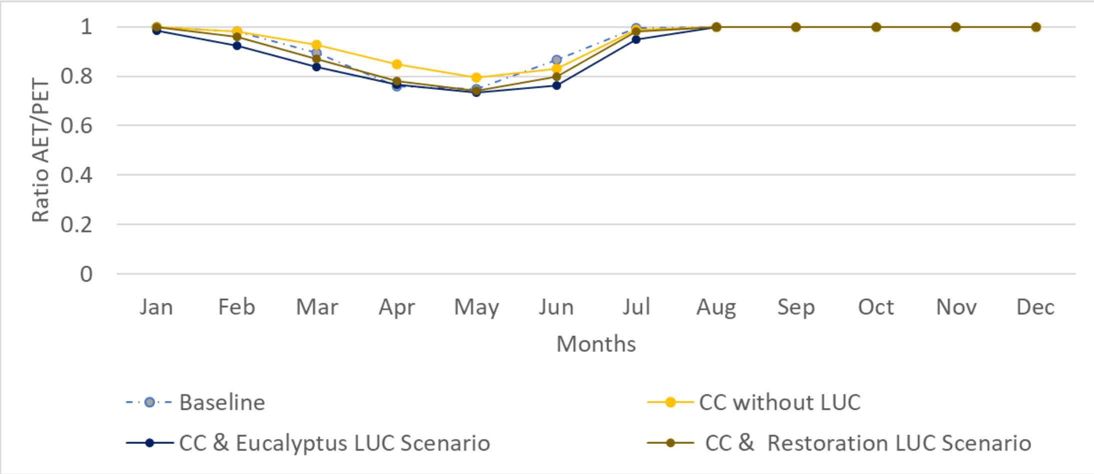

Figure 16
Simulated monthly AET/PET Ratio in Birr

3.3. AquaCrop Results

The cumulative distribution of the yields was plotted in Figures 17 and 18. The flatter curve in the Birr for Teff yields indicates higher interannual variability compared to the other plots. Overall there was no reduction in the yields of both crops in both watersheds due to changes in water availability.

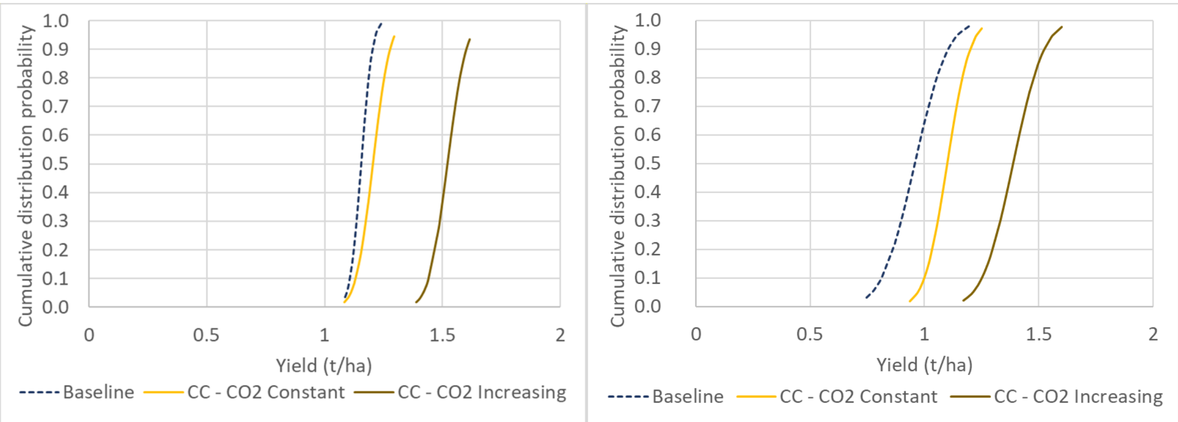

Figure 17
Cumulative distribution of Teff yields for the 30-years period in Gilgel Abbay (Right) and Birr (Left). A value of 0.9 equals 90% probability or less, while a value of 0.1 equals at least 90% probability of yields (t/ha)

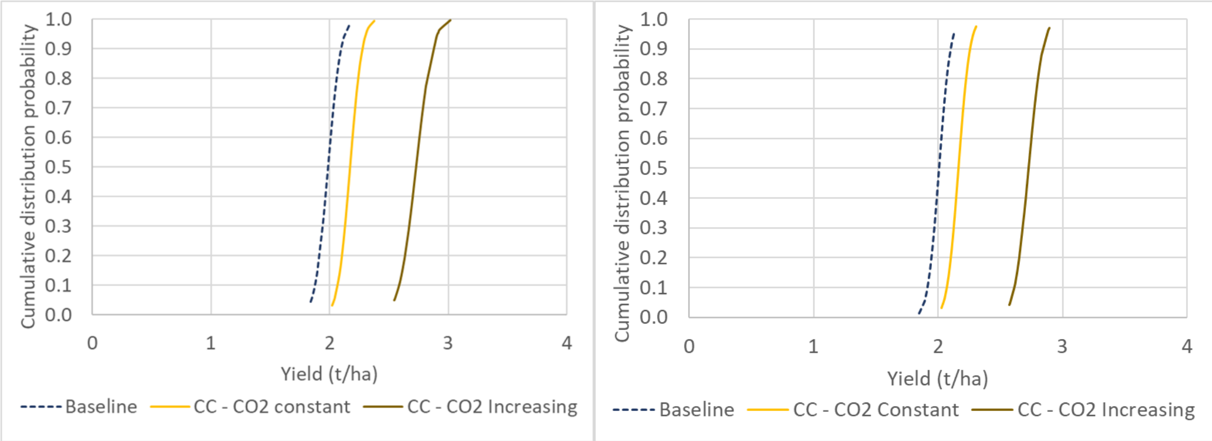

Figure 18

Cumulative distribution of Barley yields for the 30-years period in Gilgel Abbay (Right) and Birr (Left). A value of 0.9 equals 90% probability or less, while a value of 0.1 equals at least 90% probability of yields (t/ha)

4. Discussion

4.1. Climate and Land Use Change Impacts on Watershed Hydrology

The results showed that climate impacted the water balance components, and the magnitude and direction of the impacts varied across the watersheds, depending on the type and extent of LUC. Other studies have also shown similar results regarding hydrological variability due type of land uses specific to the watershed (Melesse et al., 2011; Woldesenbet & Elagib, 2021). However, CC did not seem to cause a significantly higher variability in the impacts on the hydrology compared to CC & LUC combined scenarios. This could be because the increase in rainfall predicted by the climate scenario was small, 2% in Gilgel Abbay and 3.3% in Birr. Other studies in the region with different predication for climate change scenarios have shown that the amount of rainfall increase compared to their baseline depends on the GCMs and greenhouse gases concentration scenarios. For instance, Gebre, (2015) used data from other GCMs, such as MPI and CNRM-cm5, and IPCC Representative Concentration Pathway (RCP) 4.5 scenario. The author found that the change in mean precipitation was more than 20% in the MPI RCP 4.5 prediction in Gilgel Abbay, while the CHNRM-cm5 RCP 4.5 showed a lower increase in mean precipitation, around 5%. Uncertainties of the data inputs, the downscaling approach of the GCMs and the greenhouse emissions scenarios can play a role in determining the models' outputs (Miao et al., 2023).

4.2. Seasonal Variability

CC & LUC has altered the seasonal patterns in the study watershed by increasing or decreasing the water balance components, as shown in section 3.2 of the results. The change in monthly runoff was correlated with the magnitude of the change in monthly rainfall, while the increase in the AET was more correlated with the total monthly rainfall. For instance, AET was higher in the rainy months of July and August, even though April had the highest magnitude of change increase in rainfall. This is likely because much vegetation reaches the water needs demands during the rainy season, which increases the AET.

4.3. HBV Model Representation of Land Use Scenarios

The nine parameters of 50 sets for each watershed reflected land use scenarios, as the impacts observed in other studies in the region reflected the categorisation of the land uses in this study. For instance, the results by Woldesenbet et al., (2017) show that the expansion of cultivated land and the reduction of woody shrubs in the Tana sub-basin have increased the surface runoff. In contrast, Woodland decreased runoff compared to cultivated land. This is consistent with the findings in this study. For instance, in the restoration scenario, Gilgel Abbay decreased runoff relatively higher than Birr since cultivated land increased in the restoration scenario by only 4% in GA and 14% in Birr compared to the baseline. In addition, Gilgel Abbay had a higher fraction of natural forest hypothetically restored (7%) compared to Birr, which had 5%.

4.4. Water Availability and Land Use Change

The yearly AET/PET ratio and the number of days with a maximum ratio (>0.9) were higher in the restoration scenario compared to other LUC scenarios and the baseline. This is possible mainly due to the reduced fraction of eucalyptus plantations compared to the baseline and the other LUC scenarios. Eucalyptus is known to consume high amounts of water, which may deplete water resources (Lane et al., 2004).

Birr did not have the same trend in the restoration scenario as in Gilgel Abbay, which can be explained by the fact that Birr did not have any Eucalpyutus plantations in the baseline scenario. Birr watershed was also generally less water-stressed than Gilgel Abbay since the AET/PET ratio values were high in all scenarios. Under the CC and Eucalyptus scenario, Birr had the highest reduction in the number of days with a maximum AET/PET ratio, which can imply that more plantations of Eucalyptus can lead to less water availability in the watershed.

When it comes to water storage, CC alone decreased soil water storage. With the influence of the restoration scenario, soil water storage is decreased more than in other scenarios in both watersheds. In Gilgel Abbay restoration scenario, soil water storage decreased significantly compared to other scenarios which can be due to the increased uptake of water by transpiration. In contrast, the upper and lower groundwater storage increased. The opposite was observed with the eucalyptus scenario, where water is decreased in the lower groundwater storage. The same trend was seen in Birr, where a 75% increase was observed in the upper groundwater storage but reduced lower groundwater storage by -27%. Under water stress, the roots of eucalyptus trees are able to draw water from a large area in the vicinity of its root system since they can grow even up to 6-9 m deep and extract more water (Hoogar et al., 2019) which can compete with other vegetations for water resources

The impacts of eucalyptus plantations on water resources in Ethiopia are conflicted when other factors are involved. For instance, Negasa et al., (2016) stated that Eucalyptus contributed to reducing pressure on extracting wood from natural forest cutting, which slows down deforestation in Ethiopia. Moreover, Alemayehu & Melka, (2022) concluded that eucalyptus plantations could be an excellent asset for rural development and poverty reduction in Ethiopia, and the positive impacts could outweigh the negative ones if planted on suitable sites with good management planning.

4.5. Crop Yields Predication

The purpose of this part of the study is to investigate commonly cultivated rainfed crops' response to projected climate change. The simulations were for Teff and Barley yields, assuming no other stressors, such as weed infestation or soil fertility. The only possible stressors were water stress during the growing season or high temperatures above the maximum crop threshold. The CC-induced impacts on rainfed crops had a trend of increase in yields in both watersheds based on the results of the cumulative distribution function of the different scenarios in Figures 17 and 18. Teff and Barley are usually planted in the Kiremt season, which will increase total precipitation based on the projected climate results. This can be the main factor of an increase in the investigated crop yields. However, other crops grown in different periods might be influenced differently by the changes in climatic conditions (Minta et al., 2014). It is also critical to note that an increase in yields under increased CO_2 can reduce the nutritional value and quality of the yield, which is another issue for food security (Ebi & Loladze, 2019).

5. Conclusion

Anthropogenic-induced global change drivers of land use change (LUC) and climate change (CC) substantially affect the hydrologic cycle at different scales. These events disrupt the water balance and can cause significant damage to human and natural systems, especially when the region affected is vulnerable such as the UBNB in Ethiopia. Changes in land use significantly impact water availability in studied watersheds in the periods investigated. The changes were influenced mainly by land use dynamics specific to the watershed. Based on the results presented in this paper, eucalyptus plantations negatively influenced the availability of water in Gilgel Abbay. However, in Birr the impact on water availability was not pronounced since the watershed is not water-stressed as Gilgel Abbay. Moreover, eucalyptus plantation may have consequences for groundwater resources in the long-term. Therefore, assessing the eucalyptus plantations expansion is essential to be taken into account if water resources are stressed in the region.

Under the projected CC, the investigated crops, Teff and Barley, water was not a limiting factor. This was mainly due the fact that during the growing period of the crops, precipitation increased. Additionally, CO2 would enhance the yield potential. However, crops with varied growing periods and other factors outside the report's scope such as weed infestation can influence the yields differently.

This study acknowledges the uncertainties in the models' input, models structure and aims to provide insights based on the patterns observed in the projected impacts of climate variables and land uses rather than giving precise estimates. However, due to the high variability in the impacts of land uses on water availability seen in the results, land management planning is critical for effective water-related watershed-specific adaptation strategies.

6. Bibliography

Abdo, K. S., Fiseha, B. M., Rientjes, T. H. M., Gieske, A. S. M., & Haile, A. T. (2009). Assessment of climate change impacts on the hydrology of Gilgel Abay catchment in Lake Tana basin, Ethiopia. *Hydrological Processes, 23*(26), 3661–3669. Scopus. https://doi.org/10.1002/hyp.7363

Alemayehu, A., & Melka, Y. (2022). Small scale eucalyptus cultivation and its socioeconomic impacts in Ethiopia: A review of practices and conditions. *Trees, Forests and People*, *8*, 100269. https://doi.org/10.1016/j.tfp.2022.100269

Allan, R., Pereira, L., & Smith, M. (1998). *Crop evapotranspiration-Guidelines for computing crop water requirements-FAO Irrigation and drainage paper 56* (Vol. 56).

Araya, A., Habtu, S., Hadgu, K. M., Kebede, A., & Dejene, T. (2010). Test of AquaCrop model in simulating biomass and yield of water deficient and irrigated barley (Hordeum vulgare). *Agricultural Water Management*, *97*(11), 1838–1846. https://doi.org/10.1016/j.agwat.2010.06.021

Araya, A., Keesstra, S. D., & Stroosnijder, L. (2010). Simulating yield response to water of Teff (Eragrostis tef) with FAO's AquaCrop model. *Field Crops Research*, *116*(1), 196–204. https://doi.org/10.1016/j.fcr.2009.12.010

Araya, A., Prasad, P. V. V., Jha, P. K., Singh, H., Ciampitti, I. A., & Min, D. (2023). Modeling Impacts of Climate Change and Adaptation Strategies for Cereal Crops in Ethiopia. In *Global Agricultural Production: Resilience to Climate Change* (pp. 383–408). Scopus. https://doi.org/10.1007/978-3-031-14973-3_15

Awange, J. (2022). Food Security in Blue Nile: Ethiopian GERD. In J. Awange (Ed.), *Food Insecurity & Hydroclimate in Greater Horn of Africa: Potential for Agriculture Amidst Extremes* (pp. 29–37). Springer International Publishing. https://doi.org/10.1007/978-3-030-91002-0_2

Belay, T., & Mengistu, D. A. (2019). Land use and land cover dynamics and drivers in the Muga watershed, Upper Blue Nile basin, Ethiopia. *Remote Sensing Applications: Society and Environment*, *15*, 100249. https://doi.org/10.1016/j.rsase.2019.100249

Bergström, S. (1992). *The HBV Model: Its Structure and Applications*. SMHI.

BERHE, A., Gebrekidan, A. G., DEMELASH, T., Martorano, L., Gebregzeabher, H., & Abraha, A. (2015). Assessing impacts of climate change on tef (Eragrostis tef) productivity in Debrezeit area, Ethiopia. *International Journal of Agricultural Science Research*, *3*, 1–10.

Birhanu, A., Masih, I., van der Zaag, P., Nyssen, J., & Cai, X. (2019). Impacts of land use and land cover changes on hydrology of the Gumara catchment, Ethiopia. *Physics and Chemistry of the Earth, Parts A/B/C*, *112*, 165–174. https://doi.org/10.1016/j.pce.2019.01.006

Brauman, K. A., Siebert, S., & Foley, J. A. (2013). Improvements in crop water productivity increase water sustainability and food security—A global analysis. *Environmental Research Letters*, *8*(2), 024030. https://doi.org/10.1088/1748-9326/8/2/024030

Caretta, M. A., Mukherji, A., Arfanuzzaman, M., Betts, R. A., Gelfan, A., Hirabayashi, Y., Lissner, T. K., Lopez Gunn, E., Liu, J., Morgan, R., Mwanga, S., & Supratid, S. (2022). Water. In H.-O. Pörtner, D. C. Roberts, M. M. B. Tignor, E. S. Poloczanska, K. Mintenbeck, A. Alegría, M. Craig, S. Langsdorf, S. Löschke, V. Möller, A. Okem, & B. Rama (Eds.), *Climate Change 2022: Impacts, Adaptation and Vulnerability. Contribution of Working Group II to the Sixth Assessment Report of the Intergovernmental Panel on Climate Change*. Cambridge University Press.

Conway, D. (2000). The Climate and Hydrology of the Upper Blue Nile River. *The Geographical Journal*, *166*(1), 49–62.

Crossman, J., Futter, M. N., Oni, S. K., Whitehead, P. G., Jin, L., Butterfield, D., Baulch, H. M., & Dillon, P. J. (2013). Impacts of climate change on hydrology and water quality: Future proofing management strategies in the Lake Simcoe watershed, Canada. *Journal of Great Lakes Research, 39*(1), 19–32. https://doi.org/10.1016/j.jglr.2012.11.003

Dile, Y. T., Tekleab, S., Ayana, E. K., Gebrehiwot, S. G., Worqlul, A. W., Bayabil, H. K., Yimam, Y. T., Tilahun, S. A., Daggupati, P., Karlberg, L., & Srinivasan, R. (2018). Advances in water resources research in the Upper Blue Nile basin and the way forward: A review. *Journal of Hydrology, 560*, 407–423. https://doi.org/10.1016/j.jhydrol.2018.03.042

Droogers, P., & Allen, R. G. (2002). Estimating Reference Evapotranspiration Under Inaccurate Data Conditions. *Irrigation and Drainage Systems*, *16*(1), 33–45. https://doi.org/10.1023/A:1015508322413

Dwarakish, G. S., & Ganasri, B. P. (2015). Impact of land use change on hydrological systems: A review of current modeling approaches. *Cogent Geoscience*, *1*(1), 1115691. https://doi.org/10.1080/23312041.2015.1115691

Ebi, K. L., & Loladze, I. (2019). Elevated atmospheric CO2 concentrations and climate change will affect our food's quality and quantity. *The Lancet Planetary Health*, *3*(7), e283–e284. https://doi.org/10.1016/S2542-5196(19)30108-1

FAO. (2015). *Chapter 4*. https://www.fao.org/3/x0490e/x0490e08.htm

Gebre, S. (2015). Hydrological Response to Climate Change of the Upper Blue Nile River Basin: Based on IPCC Fifth Assessment Report (AR5). *Journal of Climatology & Weather Forecasting*, *03*. https://doi.org/10.4172/2332-2594.1000121

Gebrehiwot, S. G., Bewket, W., Gärdenäs, A. I., & Bishop, K. (2014). Forest cover change over four decades in the Blue Nile Basin, Ethiopia: Comparison of three watersheds. *Regional Environmental Change*, *14*(1), 253–266. https://doi.org/10.1007/s10113-013-0483-x

Gebrehiwot, S. G., Seibert, J., Gärdenäs, A. I., Mellander, P.-E., & Bishop, K. (2013). Hydrological change detection using modeling: Half a century of runoff from four rivers in the Blue Nile Basin. *Water Resources Research*, *49*(6), 3842–3851. https://doi.org/10.1002/wrcr.20319

Getachew, B., & Manjunatha, B. R. (2021). Climate change projections and trends simulated from the CMIP5 models for the Lake Tana sub-basin, the Upper Blue Nile (Abay) River Basin, Ethiopia. *Environmental Challenges*, *5*, 100385. https://doi.org/10.1016/j.envc.2021.100385

H. Hargreaves, G., & A. Samani, Z. (1985). Reference Crop Evapotranspiration from Temperature. *Applied Engineering in Agriculture*, *1*(2), 96–99. https://doi.org/10.13031/2013.26773

Hargreaves, G. H., & Allen, R. G. (2003). History and Evaluation of Hargreaves Evapotranspiration Equation. *Journal of Irrigation and Drainage Engineering*, *129*(1), 53–63. https://doi.org/10.1061/(ASCE)0733-9437(2003)129:1(53)

Hoogar, R., Malakannavar, S., & H T, S. (2019). *Impact of eucalyptus plantations on ground water and soil ecosystem in dry regions*. *8*, 2929–2933.

Hosonuma, N., Herold, M., Sy, V. D., Fries, R. S. D., Brockhaus, M., Verchot, L., Angelsen, A., & Romijn, E. (2012). An assessment of deforestation and forest degradation drivers in developing countries. *Environmental Research Letters*, *7*(4), 044009. https://doi.org/10.1088/1748-9326/7/4/044009

Kayitesi, N. M., Guzha, A. C., & Mariethoz, G. (2022). Impacts of land use land cover change and climate change on river hydro-morphology- a review of research studies in tropical regions. *Journal of Hydrology*, *615*, 128702. https://doi.org/10.1016/j.jhydrol.2022.128702

Lane, P. N. J., Morris, J., Ningnan, Z., Guangyi, Z., Guoyi, Z., & Daping, X. (2004). Water balance of tropical eucalypt plantations in south-eastern China. *Agricultural and Forest Meteorology*, *124*(3), 253–267. https://doi.org/10.1016/j.agrformet.2004.01.015

Lemann, T., Roth, V., Zeleke, G., Subhatu, A., Kassawmar, T., & Hurni, H. (2018). Spatial and Temporal Variability in Hydrological Responses of the Upper Blue Nile basin, Ethiopia. *Water, 11*, 21. https://doi.org/10.3390/w11010021

Liu, C., Sun, G., McNulty, S. G., Noormets, A., & Fang, Y. (2017). Environmental controls on seasonal ecosystem evapotranspiration/potential evapotranspiration ratio as determined by the global eddy flux measurements. *Hydrology and Earth System Sciences*, *21*(1), 311–322. https://doi.org/10.5194/hess-21-311-2017

Loaiciga, H. A., Valdes, J. B., Vogel, R., Garvey, J., & Schwarz, H. (1996). Global warming and the hydrologic cycle. *Journal of Hydrology*, *174*(1), 83–127. https://doi.org/10.1016/0022-1694(95)02753-X

M, S., R, A., J.l, M., A, P., L, S. P., & A, S. (1992). *Report. Expert Consultation on Revision of FAO Methodologies for Crop Water Requirements.* Expert Consultation on Revision of FAO Methodologies for Crop Water Requirements. Rome (Italy). 28-31 May 1990. https://scholar.google.com/scholar_lookup?title=Report.+Expert+Consultation+on+Revision+of+FAO+Methodologies+for+Crop+Water+Requirements.&author=Smith+M.&publication_year=1992

Melesse, A. M., Abtew, W., Setegn, S. G., & Dessalegne, T. (2011). Hydrological Variability and Climate of the Upper Blue Nile River Basin. In A. M. Melesse (Ed.), *Nile River Basin: Hydrology, Climate and Water Use* (pp. 3–37). Springer Netherlands. https://doi.org/10.1007/978-94-007-0689-7_1

Mellander, P.-E., Gebrehiwot, S., Gärdenäs, A., Bewket, W., & Bishop, K. (2013). Summer Rains and Dry Seasons in the Upper Blue Nile Basin: The Predictability of Half a Century of Past and Future Spatiotemporal Patterns. *PloS One*, *8*, e68461. https://doi.org/10.1371/journal.pone.0068461

Miao, C., Wu, Y., Fan, X., & Su, J. (2023). Projections of Global Land Runoff Changes and Their Uncertainty Characteristics During the 21st Century. *Earth's Future*, *11*(4), e2022EF003286. https://doi.org/10.1029/2022EF003286

Minta, Assefa, G., & Feyissa, F. (2014). Potential of feed-food double-cropping in central highlands of Ethiopia. *Archives of Agronomy and Soil Science, 60*. https://doi.org/10.1080/03650340.2013.878456

Nachtergaele, F. O., Velthuizen, H. van, Verelst, L., Wiberg, D., Batjes, N. H., Dijkshoorn, J. A., Engelen, V. W. P. van, Fischer, G., Jones, A., Montanarella, L., Petri, M., Prieler, S., Teixeira, E., & Shi, X. (2012). *Harmonized World Soil Database (version 1.2)*. https://research.wur.nl/en/publications/harmonized-world-soil-database-version-12

Negasa, D., Mbilinyi, B., Mahoo, H., & Lemenih, M. (2016). Eucalyptus Expansion as Relieving and Provocative Tree in Ethiopia. *Journal of Agriculture and Ecology Research International*, *6*, 1–12. https://doi.org/10.9734/JAERI/2016/22841

Obengo, J. (2016). Hydropolitics of the Nile: The case of Ethiopia and Egypt. *African Security Review*, *25*, 1–9. https://doi.org/10.1080/10246029.2015.1126527

Ortiz-Bobea, A., Ault, T. R., Carrillo, C. M., Chambers, R. G., & Lobell, D. B. (2021). Anthropogenic climate change has slowed global agricultural productivity growth. *Nature Climate Change*, *11*(4), Article 4. https://doi.org/10.1038/s41558-021-01000-1

Patel, J., Patel, H., & Bhatt, C. (2015). Modified Hargreaves Equation for Accurate Estimation of Evapotranspiration of Diverse Climate Locations in India. *Proceedings of the National Academy of Sciences, India Section B: Biological Sciences*, *85*(1), 161–166. https://doi.org/10.1007/s40011-014-0314-y

Pervin, L., Gan, T. Y., Scheepers, H., & Islam, M. S. (2021). Application of the HBV model for the future projections of water levels using dynamically downscaled global climate model data. *Journal of Water and Climate Change*, *12*(6), 2364–2377. https://doi.org/10.2166/wcc.2021.302

Pidwirny, M. (2006). Actual and Potential Evapotranspiration. In *Fundamentals of Physical Geography* (2nd Edition). http://www.physicalgeography.net/fundamentals/8j.html

Pörtner, H.-O., Roberts, D. C., Adams, H., Adelekan, I., Adler, C., Adrian, R., Aldunce, P., Ali, E., Begum, R. A., Bednar-Friedl, B., Bezner Kerr, R., Biesbroek, R., Birkmann, J., Bowen, K., Caretta, M. A., Carnicer, J., Castellanos, E., Cheong, T. S., Chow, W., … Ibrahim, Z. Z. (2022). Technical summary. In H.-O. Pörtner, D. C. Roberts, M. M. B. Tignor, E. S. Poloczanska, K. Mintenbeck, A. Alegría, M. Craig, S. Langsdorf, S. Löschke, V. Möller, A. Okem, & B. Rama (Eds.), *Climate Change 2022: Impacts, Adaptation and Vulnerability. Contribution of Working Group II to the Sixth Assessment Report of the Intergovernmental Panel on Climate Change*. Cambridge University Press.

Scenario Data for the Atmospheric Environment. (n.d.). Retrieved April 23, 2023, from https://ipcc-data.org/sim/gcm_clim/SRES_TAR/ddc_sres_emissions.html

Seibert, J., & Bergström, S. (2021). *A retrospective on hydrological modelling based on half a century with the HBV model*. https://doi.org/10.5194/hess-2021-542

Seibert, J., & Vis, M. J. P. (2012). Teaching hydrological modeling with a user-friendly catchment-runoff-model software package. *Hydrology and Earth System Sciences*, *16*(9), 3315–3325. https://doi.org/10.5194/hess-16-3315-2012

Speich, M. J. R. (2019). Quantifying and modeling water availability in temperate forests: A review of drought and aridity indices. *IForest - Biogeosciences and Forestry*, *12*(1), 1. https://doi.org/10.3832/ifor2934-011

Spitters, C. J. T. (1990). CROP GROWTH MODELS: THEIR USEFULNESS AND LIMITATIONS. *Acta Horticulturae*, *267*, 349–368. https://doi.org/10.17660/ActaHortic.1990.267.42

Steele-Dunne, S., Lynch, P., McGrath, R., Semmler, T., Wang, S., Hanafin, J., & Nolan, P. (2008). The impacts of climate change on hydrology in Ireland. *Journal of Hydrology*, *356*(1), 28–45. https://doi.org/10.1016/j.jhydrol.2008.03.025

Te Wierik, S. A., Keune, J., Miralles, D. G., Gupta, J., Artzy-Randrup, Y. A., Gimeno, L., Nieto, R., & Cammeraat, L. H. (2022). The Contribution of Transpiration to Precipitation Over African Watersheds. *Water Resources Research*, *58*(11), e2021WR031721. https://doi.org/10.1029/2021WR031721

Teklay, A., Dile, Y. T., Asfaw, D. H., Bayabil, H. K., & Sisay, K. (2021). Impacts of Climate and Land Use Change on Hydrological Response in Gumara Watershed, Ethiopia. *Ecohydrology & Hydrobiology*, *21*(2), 315–332. https://doi.org/10.1016/j.ecohyd.2020.12.001

Trisos, C. H., Adelekan, I. O., Totin, E., Ayanlade, A., Efitre, J., Gemeda, A., Kalaba, K., Lennard, C., Masao, C., Mgaya, Y., Ngaruiya, G., Olago, D., Simpson, N. P., & Zakieldeen, S. (2022). Africa. In H.-O. Pörtner, D. C. Roberts, M. M. B. Tignor, E. S. Poloczanska, K. Mintenbeck, A. Alegría, M. Craig, S. Langsdorf, S. Löschke, V. Möller, A. Okem, & B. Rama (Eds.), *Climate Change 2022: Impacts, Adaptation and Vulnerability. Contribution of Working Group II to the Sixth Assessment Report of the Intergovernmental Panel on Climate Change*. Cambridge University Press.

van Luijk, G., Cowling, R. M., Riksen, M. J. P. M., & Glenday, J. (2013). Hydrological implications of desertification: Degradation of South African semi-arid subtropical thicket. *Journal of Arid Environments*, *91*, 14–21. https://doi.org/10.1016/j.jaridenv.2012.10.022

Vanuytrecht, E., Hsiao, T., Fereres, E., Heng, L., García-Vila, M., & Mejías, P. (2014). AquaCrop: FAO'S crop water productivity and yield response model. *Environmental Modelling and Software*, *62*. https://doi.org/10.1016/j.envsoft.2014.08.005

WaleWorqlul, A., Taddele, Y. D., Ayana, E. K., Jeong, J., Adem, A. A., & Gerik, T. (2018). Impact of climate change on streamflow hydrology in headwater catchments of the upper Blue Nile Basin, Ethiopia. *Water (Switzerland)*, *10*(2), Article 2. https://doi.org/10.3390/w10020120

Water Hydro Diplomacy And Communication Forum Documents | Ministry of Water and Energy. (n.d.). Retrieved April 25, 2023, from https://mowe.gov.et/en/resource_types/water-hydro-diplomacy-and-communication-forum-documents-

WMO Guidelines on the Calculation of Climate Normals. (2021, August 20). https://public.wmo.int/en/resources/library/wmo-guidelines-calculation-of-climate-normals

Worqlul, A. W., Collick, A. S., Rossiter, D. G., Langan, S., & Steenhuis, T. S. (2015). Assessment of surface water irrigation potential in the Ethiopian highlands: The Lake Tana Basin. *CATENA*, *129*, 76–85. https://doi.org/10.1016/j.catena.2015.02.020

Yao, A. Y. M. (1974). Agricultural potential estimated from the ratio of actual to potential evapotranspiration. *Agricultural Meteorology*, *13*(3), 405–417. https://doi.org/10.1016/0002-1571(74)90081-8

Yitayew, M., & Melesse, A. M. (2011). *Critical Water Resources Issues in the Nile River Basin* (A. M. Melesse, Ed.; pp. 401–416). Springer Netherlands. https://doi.org/10.1007/978-94-007-0689-7_20

7. Appendices

7.1. Appendix 1: Crop Characteristics Parameters

- **Conservative Crop Parameters**

No.	Conservative Crop Parameters	Teff	Barley
1	Soil water depletion factors (p) are adjusted by ETo	1	1
2	Base temperature (°C) below which crop development does not progress	10	0
3	Upper temperature (°C) above which crop development no longer increases with an increase in temperature	30	15
4	Soil water depletion factor for canopy expansion (p-exp) - Upper threshold	0.32	0.20
5	Soil water depletion factor for canopy expansion (p-exp) - Lower threshold	0.66	0.65
6	Shape factor for water stress coefficient for canopy expansion	3	3
7	Soil water depletion fraction for stomatal control (p - sto) - Upper threshold	0.60	0.60
8	Shape factor for water stress coefficient for stomatal control	3	3
9	Soil water depletion factor for canopy senescence (p - sen) - Upper threshold	0.58	0.55
10	Shape factor for water stress coefficient for canopy senescence	3	3
11	Sum(ETo) during dormant period to be exceeded before crop is permanently wilted	50	50
12	Soil water depletion factor for pollination (p - pol) - Upper threshold	0.92	0.85
13	Vol% for Anaerobiotic point (* (SAT - [vol%]) at which deficient aeration occurs *)	6	15
14	Considered soil fertility stress for calibration of stress response (%)	34	50
15	Minimum air temperature below which pollination starts to fail (cold stress) (°C)	8	5
16	Maximum air temperature above which pollination starts to fail (heat stress) (°C)	40	35
17	Minimum growing degrees required for full crop transpiration (°C - day)	11.1	14
18	Electrical Conductivity of soil saturation extract at which crop starts to be affected by soil salinity (dS/m)	2	6
19	Electrical Conductivity of soil saturation extract at which crop can no longer grow (dS/m)	12	20
20	Calibrated distortion (%) of CC due to salinity stress (Range: 0 (none) to +100 (very strong))	25	25
21	Calibrated response (%) of stomata stress to ECsw (Range: 0 (none) to +200 (extreme))	100	100
22	Crop coefficient when canopy is complete but prior to senescence (KcTr,x)	1.10	1.10

23	Decline of crop coefficient (%/day) as a result of ageing, nitrogen deficiency, etc.	0.300	0.150
24	Minimum effective rooting depth (m)	0.30	0.30
25	Maximum effective rooting depth (m)	0.60	1.30
26	Shape factor describing root zone expansion	15	15
27	Maximum root water extraction (m3water/m3soil.day) in top quarter of root zone	0.048	0.048
28	Maximum root water extraction (m3water/m3soil.day) in bottom quarter of root zone	0.012	0.012
29	Effect of canopy cover in reducing soil evaporation in late season stage	60	50
30	Soil surface covered by an individual seedling at 90% emergence (cm2)	0.25	1.5
31	Canopy size of individual plant (re-growth) at 1st day (cm2)	0.25	1.5
32	Number of plants per hectare	10,000,000	1,500,000
33	Canopy growth coefficient (CGC): Increase in canopy cover (fraction soil cover per day)	0.14644	0.12410
34	Maximum canopy cover (CCx) in fraction soil cover	0.81	0.80
35	Canopy decline coefficient (CDC): Decrease in canopy cover (in fraction per day)	0.11600	0.07697
36	Calendar Days: from sowing to emergence	14	7
37	Calendar Days: from sowing to maximum rooting depth	55	60
38	Calendar Days: from sowing to start senescence	75	65
39	Calendar Days: from sowing to maturity (length of crop cycle)	99	93
40	Calendar Days: from sowing to flowering	55	60
41	Length of the flowering stage (days)	11	12
42	Crop determinacy linked with flowering	1	1
43	Excess of potential fruits (%)	50	100
44	Building up of Harvest Index starting at flowering (days)	40	27
45	Water Productivity normalized for ETo and CO_2 (WP*) (gram/m2)	14	15
46	Water Productivity normalized for ETo and CO_2 during yield formation (as % WP*)	100	100
47	Crop performance under elevated atmospheric CO_2 concentration (%)	50	50

48	Reference Harvest Index (HIo) (%)	27	33
49	Possible increase (%) of HI due to water stress before flowering	0	5
50	Coefficient describing positive impact on HI of restricted vegetative growth during yield formation	0.5	10
51	Coefficient describing negative impact on HI of stomatal closure during yield formation	10	10
52	Allowable maximum increase (%) of specified HI	40	15
53	dry matter content (%) of fresh yield	90	90

- **Non-conservative Crop Parameters**

Parameters affected by Planting/Management	**Teff**	**Barley**
Type of Planting Method (Direct sowing or Transplanting)	Direct sowing	Direct sowing
Plant density – Initial Canopy cover (CCo) at 90% emergence	Estimated with sowing rate if 24.43 kg seed/ha for a 1000 seed mass of 2.85 and a germination rate of 70% CCo1.5%	Estimated with sowing rate if 9.66 kg seed/ha for a 1000 seed mass of 2.85 and a germination rate of 70% CCo 3.56%
Plant density – Maximum Canopy cover (CCx) in the mid growing season	81% well covered	80% well covered
Time to emergence	14 days	7 days

Cultivar specific parameters	**Teff**	**Barley**
Time to maximum canopy cover	55 days	56 days
Time to the beginning of canopy senescence	75 days	65 days
Time to physiological maturity	99 days	93 days
Time to start flowering or the start of yield formation	55 days	60 days
Duration of flowering	11 days	12 days

Parameters affected by conditions in the soil profile	**Teff**	**Barley**
Time to maximum rooting depth	55 days	60 days
Maximum rooting depth	0.60 m (shallow – medium rooted) with an average root zone expansion of 0.8 cm/day	1.30 m (medium-rooted crops) with an average root zone expansion of 1.9 cm/day